Electrostatic control of macrocyclization reactions within nano-spaces

Kaiya Wang,^{1†} Xiaoyang Cai,^{1†} Wei Yao,¹ Du Tang,² Rhea Kataria,¹ Henry S. Ashbaugh,² Larry D Byers,¹ and Bruce C. Gibb¹.

¹Department of Chemistry, Tulane University, New Orleans, LA, 70118 ²Department of Chemical and Biomolecular Engineering, Tulane University, New Orleans, LA, 70118

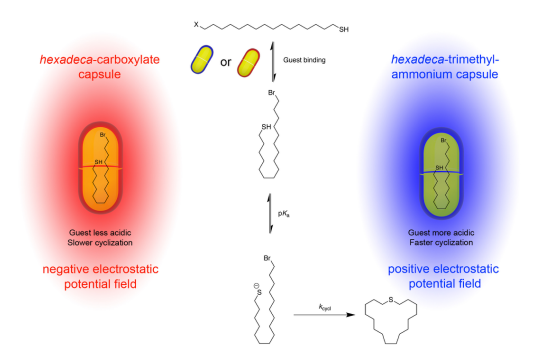
[†] KW performed initial studies into the described system. KW and XC performed the reported rate and guest motif determinations. XC performed the reported p K_a determinations, kinetic confirmation of p K_a of bound guest **2a**, and the Eyring analyses.

^{*} Corresponding author: email: bgibb@tulane.edu

Abstract

The intrinsic structural complexity of proteins makes it hard to identify the contributions of each non-covalent interaction behind the remarkable rate accelerations of enzymes. Coulombic forces are evidently primary, but despite developments in artificial nano-reactor design, a picture of the extent to which these can contribute has not been forthcoming. Here we report on two supramolecular capsules that possess structurally identical inner-spaces that differ in the electrostatic potential field (EPF) that envelops them: one positive, one negative. This architecture means that only changes in the EPF influence the chemical properties of encapsulated species. We quantify these influences via acidity and rates of cyclization measurements for encapsulated guests, and confirm the primary role of Coulombic forces with a simple mathematical model approximating the capsules as Born spheres within a continuum dielectric. These results reveal the reaction rate accelerations possible under Coulombic control and highlight important design criteria for nano-reactors.

Graphical Abstract



Introduction

Although there is still disagreement regarding how all the different non-covalent (and covalent) factors contribute to the remarkable rate accelerations observed in enzymes, 1,2 it is generally accepted that modulation of the local electrostatic potential (EP, ϕ) around the substrate has a primary role in transition state stabilization. 3,4

For some time now, chemists have examined different ways in which reactions can be controlled by EP modulation. For example, by taking advantage of the dissimilar supramolecular properties of Li⁺ and ClO₄⁻ ions, simple rearrangements or elimination reactions in diethyl ether can be greatly accelerated by high concentrations (~5 M) of LiClO₄.⁵ Building on this type of early work, more recently there has been increasing interest in using oriented external electric fields to exert precise control of non-redox reactions.⁶

Over the last decade supramolecular chemistry has become increasingly proficient at using encapsulation to control stoichiometric as well as catalytic reactions.⁷⁻¹² Regarding the former, covalent hosts, ¹³⁻¹⁷ as well as supramolecular containers assembled via the hydrophobic effect, ¹⁸⁻²¹ metal coordination, ²²⁻²⁵ and hydrogen bonding; ²⁶ have all been utilized. Regarding catalysis, supramolecular containers assembled via metal coordination have dominated to date, ²⁷⁻³⁶ but hydrogen bonded containers have also proven exceptionally successful. ³⁷⁻⁴³

These advancements noted, to our knowledge one area not systematically explored is how the specific control of the EP field within nano-containers can affect reactions. There are two principal factors as to why this is so. First, work in organic solvents has involved uncharged hosts devoid of significant EP fields. Second, although work with water-soluble hosts has involved a diversity of charge-state (-12 to +12) and hence a wide range of EP fields, these different examples have involved a wide variety of structures that make direct comparison difficult. As a step towards understanding how the specific control of the EP field within nano-containers can affect reactions we describe here the reactivity of guests within the dimeric supramolecular capsules formed by octa-carboxylate 1a and positand 1b (Figure 1). More specifically, we demonstrate that although the binding sites of capsules $1a_2$ and $1b_2$ are essentially identical, pK_a values of encapsulated thio-alkanes and the rates of cyclization of α , ω thio-alkane halides are greatly affected by the EP field of the capsule. The results demonstrate the power of Coulombic forces to influence reactions, even when charge groups are remote and fully water solvated within a high dielectric medium. Hence, they shed further light on the contributing factors to enzyme catalysis and reveal new strategies in enzyme mimicry using less complex model systems.

Results and Discussion

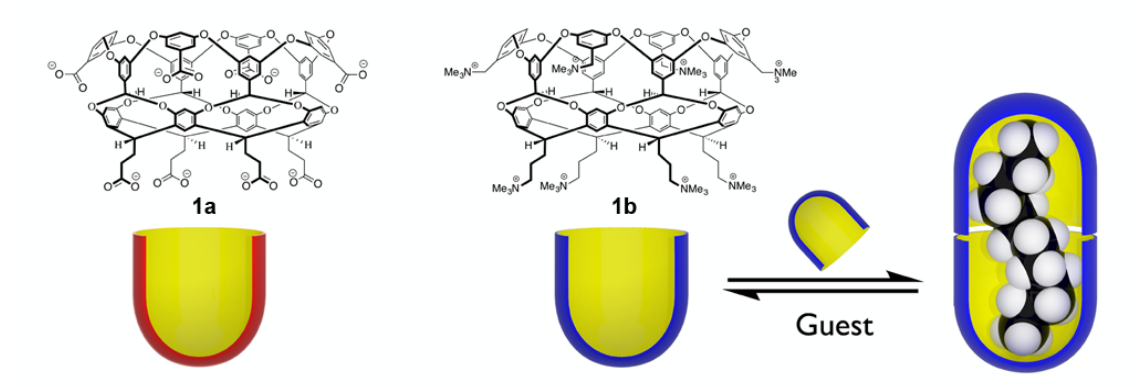


Figure 1: Hosts utilized in this study, octa-carboxylate **1a** and positand **1b**. As illustrated by host **1b**, both hosts dimerize around guests to form supramolecular nano-capsules.

Cavitands **1a** and **1b** assemble via the hydrophobic effect to form dimeric nano-capsules (Figure 1). The frameworks of these hosts are identical; as are the walls of their inner spaces and the shape and volume they define. Only their exterior coats differ; under basic conditions the external coating of **1a**₂ is nominally hexadeca-anionic, whereas **1b**₂ is hexadeca-cationic. The inner space of either capsule is nominally a dry nano-enviroment, however water does solvate empty **1a**, however water does solvate an enter a capsular complex of guest@**1a**₂ via a partial opening, or breathing, mechanism. In combination, these results suggest that the inner-space is quite heterogeneous; it is more polar at the equatorial region than the poles. The solubilizing groups of each host are > 1 nm away from the center of their inner spaces. Consequently, the only "direct" influence the charge groups can exert upon encapsulated guests is the Coulombic force intrinsic to the EP field they generate.

It has been previously shown that encapsulation of flexible guests inside containers can force them to adopt high energy U- or J-motifs possessing reverse turns within their main-chain, $^{14,54-59}$ and this phenomenon has been used to enhance cyclizations within 1:1 complexes. 14,17,60 Thus to demonstrate the role of EP fields, we report here on the encapsulation of α,ω thio-alkane halides, their deprotonation, and their cyclization to the corresponding 13- to 19-membered thio-ethers (Figure 2).

Guest Synthesis and Encapsulation

Of the six guest substrates (Figure 2a), **2a**, **2b**, and **4** were previously reported. These, and the other three novel substrates **3a/b** and **5** were synthesized as described (SI). Non-cyclizing guests **2c**, **3c** and **4b** were commercially available.

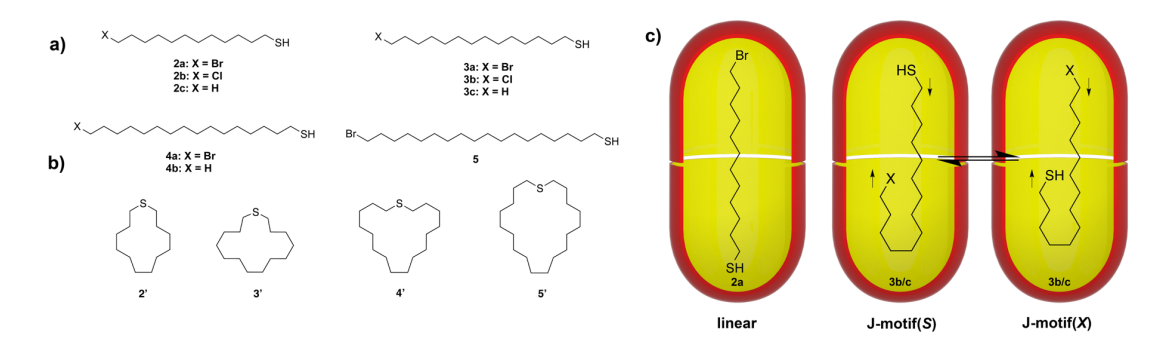


Figure 2: a) Structures of long-chain thiols **2-5** used in this study. b) The cyclic thio-ethers **2'-5'** formed within the containers **1a**₂ or **1b**₂. c) Examples of the observed binding motifs of guests using **2a** and **3b/c** as examples: **2a** in a linear motif, and **3b/c** in an equilibrium between J-motif(*S*) and J-motif(*X*).

¹H NMR spectroscopy was used to examine guest binding to capsules **1a**₂ and **1b**₂ in either D₂O or, to observe the bound thiol –SH signal, H₂O (Figures S8-S40). With the exception of minor changes to the guest binding region the only difference observed between the hosts was that **1b**₂ tended to form weaker complexes, such that larger guests were not fully bound.⁷⁰

Binding was confirmed by distinctive, high-field signals in the 1H NMR spectra of each complex. Prior NMR spectroscopy work 14 and Gauge Invariant Atomic Orbital calculations 71 have confirmed these high-field signals arise because the guest is held close to the diamagnetic, shielding walls of the container, whilst the wide anisotropy arises from the average location of a guest proton within the capsule. Determining this location utilized COSY NMR spectroscopy to assign the signals for free and bound guests and calculating the differences between these ($\Delta\delta$). As a rule-of-thumb, because each pocket is conical, the deeper an atom is located the more upfield shifted is its signal. This protocol revealed that both capsules induced the same motif in each guest, and that overall two, principal motifs were observed (Figure 2c). Shorter guests 2a/b/c and 3c were found to bind primarily in a linear motif, whereas longer guests adopted a J-motif(S) with either the thiol terminus bound deeply into a "pole", or the opposite J-motif(S) with the X group bound deeply. $\Delta\delta$ plots suggest that for both S and S the J-motif(S) predominates, but that the proportion of the J-motif(S) is higher in S Despite difficulty in assigning all of the signals of bound guests S and S hased on the much larger signal shifts of the protons at the thiol terminus these too were also assigned as J-motifs(S).

Guest Cyclization and Acidity with Capsules 1a2 and 1b2

The musk fragrance⁷² products **2'-5'** have been reported previously, but yields ranged from low to trace.⁶¹⁻⁶⁴ Unsurprisingly, in an control experiment using a dilute solution of **3a** in

basic aqueous methanol, MALDI-TOF analysis revealed that the majority of the product was random, insoluble polymer (Figure S135).

Table 1: Reaction times and apparent first order rate constants for the cyclization of guests **2a-5a** encapsulated within the capsular hosts **1a**₂ and **1b**₂^a

	Host 1a		Host 1b	
Guest	Reaction time	Rate Constant	Reaction	Rate Constant
		(k, s^{-1})	time	(k, s^{-1})
2a	> 27 d.	8.65 × 10 ⁻⁷	~ 6 min	6.60 × 10 ⁻³
2b	> 60 d	_ c	24 h	1.80 × 10 ⁻⁵
3a	~ 8 h	1.28 × 10 ⁻⁴	< 2 min	_ b
3b	> 60 d	_ c	3 h	2.50×10^{-4}
4a	42 h	2.14 × 10 ⁻⁵	< 2 min ^d	_ d
5	~ 10 d	3.85 ×10⁻ ⁶	~2 min ^e	_ e

 $^{^{\}rm a}$ All experiments were performed with 1.0 mM host 1a in 8 mM NaOH/D2O buffer or 1.0 mM host 1b in D2O at 25 $^{\rm o}$ C, with the reactions initiated by the addition of excess NaOH to give a 200 mM solution. $^{\rm b}$ Reaction too rapid to determine kinetics by $^{\rm 1}$ H NMR spectroscopy. $^{\rm c}$ Apparent first order rate not determined. $^{\rm d}$ The product was formed during complex formation (no addition of base necessary). $^{\rm e}$ Complex NMR spectra of mixture precluded detailed analysis.

The standard procedure for initiating cyclization was the addition of NaOH to a 2:1 host-guest complex to give a base concentration of 200 mM (versus 1 mM complex). However, one complex with $1b_2$ cyclized spontaneously upon mixing of host and guest (*vide infra*). In all cases cyclization was apparent by ¹H NMR spectroscopy (Figures S41-S48), and product formation was confirmed by extraction and analysis by GC-MS and NMR spectroscopy (Figures S57-S61). Yields were quantitative, and analysis revealed that products 2'-5' adopt a motif in which the S–atom resides in a "polar" region of the capsule (Figures S62-S67).

All substrates cyclized with apparent first-order kinetics. Table 1 presents the reaction time for each host-guest combination, and where it could be readily determined, the rate constant. Inside host $1a_2$, the shortest guests 2a and 2b underwent very slow reaction, and within this pair the chloro derivative 2b reacted the slowest. Guests 3a and 3b behaved analogously, with 3a reacting sufficiently quickly for a rate constant to be readily determined but 3b reacting very slowly. Interestingly, guest 3a cyclized 150 times faster than 2a. We attribute this increase rate for the bigger macrocycle to the fact that 2a adopts a linear motif in which the reacting termini reside cannot readily react, whereas bound 3a exists in J-motifs that are preorganized (templated) by the host to undergo cyclization. Guest 4a and 5a were respectively found to cyclize six and thirty-three times more slowly than 3a, suggesting steric hinderance became an issue.

Table 1 also shows that cyclizations within positively charged $1b_2$ occur much more quickly (7600 times quicker in the case of 2a). From the limited data it is evident that guests with linear motifs and chloride leaving groups reacted more slowly than longer brominated guests. For example, based on reaction times 2a cyclized 370 times faster than chloride 2b, whilst the rate constant of cyclizing 3b was found to be 26 times greater than that of 2b. The cyclization rates of thiols 3a and 4a within $1b_2$ were both too fast to monitor, with the cyclization of 4a spontaneous without the addition of base. Because of partial complexation, 1H NMR spectroscopy could not be used to accurately monitor the formation of 5 by $1b_2$, however reaction was rapid and spontaneous.

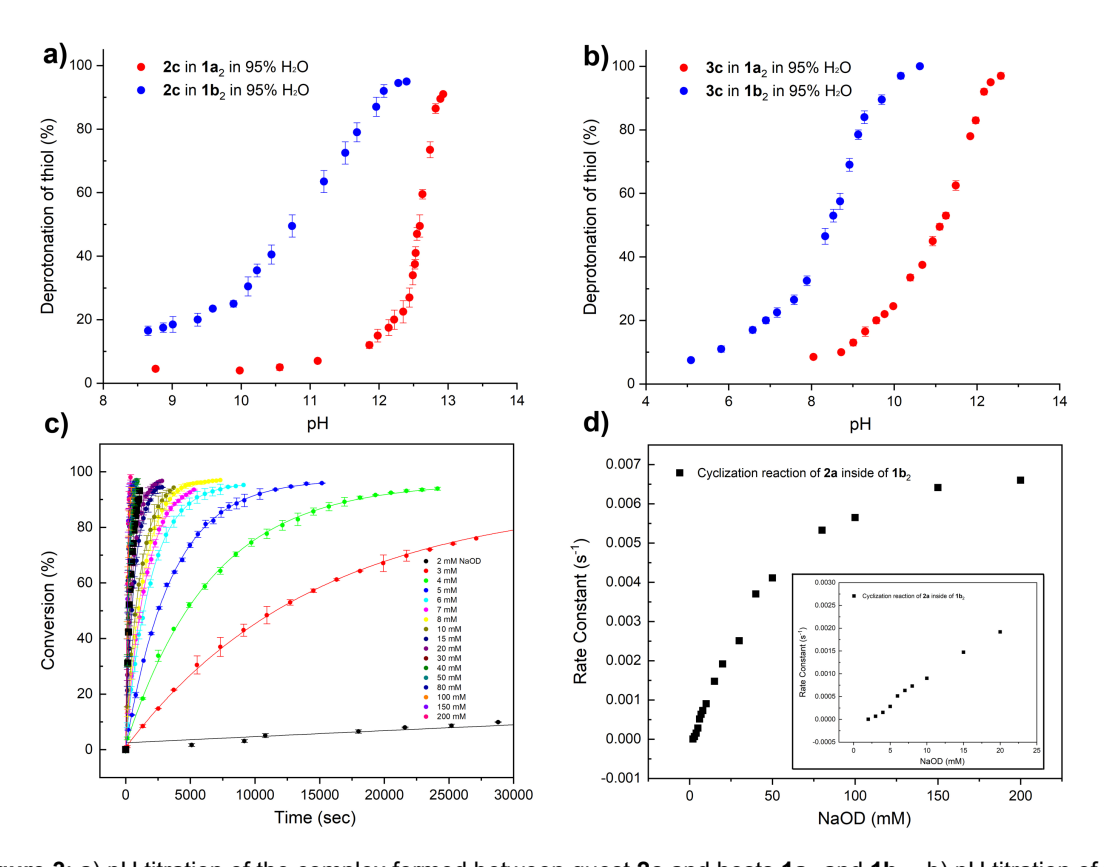


Figure 3: a) pH titration of the complex formed between guest **2c** and hosts **1a**₂ and **1b**₂. b) pH titration of the complex formed between guest **3c** and hosts **1a**₂ and **1b**₂. c) Graphs of the rate of cyclization of **2a** within the **1b**₂ capsule as a function of NaOD concentrations from 2-200 mM. d) Calculated apparent first-order rate constants for the cyclization of **2a** inside **1b**₂ as a function of [NaOD] from 2-200 mM. Inset, calculated apparent first-order rate constants as a function of [NaOH] from 2-18 mM.

To probe the effects of encapsulation on acidity, we determined the pK_a values for non-cyclizing guests **2c**, **3c** and **4b** inside the two capsules by titrating the complexes with NaOH and using ¹H NMR spectroscopy to monitor the disappearance of the bound SH signal between -1.9

and -2.8 ppm (95:5 H₂O:D₂O, Figures S103-S113). These experiments revealed that deprotonation did not lead to decomplexation or even to changes in binding motif. The titration curves for **2c** (Figure 3a) reveal p K_a values inside **1a**₂ and **1b**₂ of 12.6 and 10.7 \pm 0.1 respectively. This compares to the typical p K_a of a thiol of ~10-11. Thus, a switch from negative to positive capsule increases the acidity two orders of magnitude, but the non-polar inner-space of 1b2 counters any energetic benefits of placing the thiol in the positive EP field. Guest 3c inside 1a2 and $1b_2$ was more acidic: $pK_a = 11.2$ and 8.5 ± 0.1 respectively (Figure 3b). Why this increase? The flatter titration curves of **3c** relative to **2c** when bound to $1a_2$ (Figures 3b versus 3a), and the broader signals in the COSY NMR spectra of the 3c complex (Figures S30 versus S17) suggest that whereas 2c only adopts a linear motif, longer 3c adopts this, and to a small extent, a J-motif as well. In such a J-motif, an S-atom at the more solvent-exposed equatorial region of the capsule would be more hydrated and therefor more acidic. For guest 4b it was not possible to obtain a sufficiently clean NMR spectrum for a titration inside 1b₂, but within 1a₂ the titration yielded a weak inflection suggestive of the guest adopting multiple motifs with an average p K_a of ~9.0 (Figure S113). Overall, these results show that the pK_a of the bound thiol is enhanced by both a positive EP field and increasing guest length. Thus, the spontaneous reactivity of 4a can in part be attributed to a low p K_a value inside $1b_2$. Importantly, these titrations also reveal two key points: 1) irrespective of the host, 200 mM NaOH is sufficient for full deprotonation of all guests; 2) the average $\Delta p K_a$ between the **2c** in **1a**₂ and **1b**₂ and the corresponding complexes with **3c** is 2.3 units, corresponding to a stabilization within $1b_2$ relative to $1a_2$ of 13 kJ mol⁻¹ ($\Delta\Delta G = 2.3RT\Delta pK_a$).

Complete deprotonation at 200 mM NaOH was also confirmed kinetically for guest 2a within $1b_2$. Figure 3c and 3d shows the data for the cyclization as a function of base concentration. At all concentrations data fitted an apparent first order reaction (Figures 3c and S68 – S102), and in totality (Figure 3d) the data showed the rate constant increase saturating at 150 mM NaOD (pD \sim 12.7) commensurate with the full deprotonation of a group of p K_a 10.7 (\sim 11.1 corrected for deuterium 73). Interestingly, the data also showed an attenuation of the rate constant at low concentration of NaOD (see Figure 3d inset), a phenomenon that we attribute to OD $^-$ binding to the exterior of the capsule 52 and being unavailable for guest deprotonation.

The combination of the data shown in Table 1 and Figure 3 revealed a rather confined area of chemical-space for Eyring determinations. Nevertheless, it was possible to determine the thermodynamic parameters for three complexes (Table 2) in the presence of 200 mM NaOD: guest **2a** inside **1a**₂ (329-349 K, Figure S114 – S120), **2a** inside **1b**₂ (278-282 K, Figure S121 – S127), and guest **3a** inside **1a**₂ (305 K-322 K, Figure S128 – S134).

The difference between the cyclization inside capsules 1a₂ and 1b₂ is stark; the half-life

for cyclization of ${\bf 2a}$ is 3.5×10^3 times shorter in the positive capsule. Alternatively, the free energy of activation (ΔG^{\ddagger}) for the cyclization of ${\bf 2a}$ is over 20 kJ mol⁻¹ lower in positive ${\bf 1b}_2$ than in ${\bf 1a}_2$. This compares to the 13 kJ mol⁻¹ of stabilization for deprotonating guests in ${\bf 1b}_2$ versus ${\bf 1a}_2$. Interestingly, this demonstrates that relative to the ${\bf 1a}_2$, positive capsule ${\bf 1b}_2$ stabilizes the transition state (TS) more than it does deprotonation. The ΔH^{\ddagger} for cyclization in capsule ${\bf 1b}_2$ is over ~25 kJ mol⁻¹ lower than in ${\bf 1a}_2$, whereas the $-T\Delta S^{\ddagger}$ from the bound, deprotonated ${\bf 2a}$ to its TS is similar for both complexes. This emphasizes that the majority of the rate acceleration seen within ${\bf 1b}_2$ arises from enthalpic effects induced by the EP field.

Table 2: Thermodynamic parameters and reaction half-lives determined by Eyring analysis for selected cyclizations inside the capsules **1a**₂ and **1b**₂ (200 mM NaOH).

Guest	2a in 1a₂	2a in 1b₂	3a in 1a₂
ΔG^{\ddagger} (kJ mol ⁻¹)	105.4	84.9	95.4
ΔH^{\ddagger} (kJ mol ⁻¹)	82.0	57.7	74.9
$-T\Delta S^{\ddagger}$ (kJ mol ⁻¹)	23.4	27.2	20.5
Half-life (s, 298 K)	3.2 ×10 ⁵	93	4.8 ×10 ³

The comparison of the cyclization of guests 2a and 3a inside $1a_2$ is equally as revealing. The ΔG^{\ddagger} of cyclization of the 3a is 10 kJ mol⁻¹ lower than 2a; an effect that is again dominated by enthalpy and aided by a slightly smaller $-T\Delta S^{\ddagger}$ term. We believe the differences between cyclizing 2a and 3a stem from the fact that the two termini of linear-bound 2a must overcome anchoring to the 'poles' of the inner-space to approach each other, whereas with J-motif 3a only one terminus must "detach" from the inner wall of the host to meet the other end of the guest.

Electrostatic Potential and Transition State Stabilization Calculations

To confirm the extent to which Coulombic forces can be expected to influence reactions in $1a_2$ and $1b_2$, we turned to calculations and first evaluated the spatial EP (φ) of each capsule *in vacuo*. Figure 4a shows the cylindrically averaged φ values obtained by rotating each capsule around its C_4 axis. The EP fields about each are very similar, largely differing only in their respective signs; in the interior of the capsules the EPs are comparable in magnitude (~20 V or 778 kT/e (kT/e = 25.7 mV)) and nearly uniform, whilst outside both capsules the magnitude of the EP decays inversely with distance. As expected, the greatest distinction between the two capsules is on their outer surfaces. Encapsulated guests do not contact this boundary region, confirming that the guest to charge-group distances are short enough that guests can be greatly influenced by them, but long enough such that this influence is purely Coulombic.

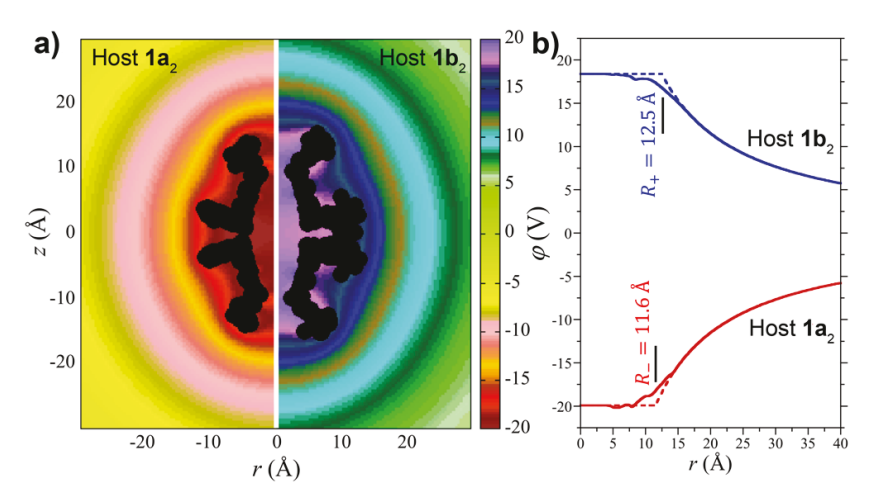


Figure 4: a) Electrostatic potential (EP, φ in volts) about (one half of) the empty capsule $\mathbf{1a}_2$ (left) and $\mathbf{1b}_2$ (right) *in vacuo*. The perspective is from the equatorial horizontal plane () perpendicular to the principal C₄ axis of the capsules. The EP is cylindrically averaged about the C₄. The net charge on each capsule is ±16e. The black shadow indicates the positions of the heavy atoms of each capsule. The EP scale is reported in the legend on the right-hand side of the figure. b) EP about host $\mathbf{1a}_2$ (red lines) and $\mathbf{1b}_2$ (blue lines) *in vacuo*, spherically averaged about the central of mass of each capsule. The solid lines indicate the mean EP determined from averaging interactions over the explicit partial charges of each capsule, while the dashed lines indicate the approximate potential distribution determined by spreading the net charge of each capsule on a sphere of radius $R_{+/-}$ (Eq. (1)). The effective Born radii of the capsules are $R_+ = 12.5$ Å and $R_- = 11.6$ Å, respectively. The mean Born radius of the hosts is $R_- = 12.0$ Å.

An alternative perspective is to plot the mean potential distribution as a function of distance from the capsules (Figure 4b). This clearly shows the uniformity of the EP inside the hosts, the inverse dependence of the EP on distance outside the capsules, and the subtle differences between the capsules at or close to their surfaces.

Because of the uniformity of φ within the capsules, we assumed that the EP fields can be semi-quantitatively described by approximating each dimer to a sphere, whose net charge of q_{\pm} = \pm 16 e is uniformly smeared over its surface at an effective radius R_{+} , Eq. (1):

$$\varphi(r) = \begin{cases} \frac{q_{\pm}}{R_{\pm}} & r \le R_{\pm} \\ \frac{q_{\pm}}{r} & r > R_{\pm} \end{cases}$$
 (1)

where r is the radial distance from the center of the capsule, and R_{\pm} is the Born radius of each capsule (the effective container size that demarks the boundary between the interior and the bulk solvent modeled as a continuum dielectric): $R_{-} = 11.6$ Å and $R_{+} = 12.5$ Å for capsules $1a_{2}$ and $1b_{2}$, respectively. The main difference between the cylindrical averaged potentials and the picture emerging from approximating Eq. (1) is again near R_{+} (Figure 4b). Thus, treating the capsules

as spheres is a valid approximation for evaluating the effect of EP on bound charged species.

While this simple model is an excellent approximation, it does not capture the significant role of water. Solvation shell waters on the exterior of the container are polarized by the \pm 16 e charge on the surface. As a result, the charge on the surface of the host is strongly attenuated and there is a corresponding reduction of the inner EP by approximately a factor of 78 (ϵ , the dielectric of water) to \sim 250 mV or 9.7 kT/e. In addition, any added electrolyte further screens interactions by counterion redistribution in the field of the capsules. To account for these effects in our model we treated water as a dielectric continuum, and approximated the counter-ion effect within the context of Debye-Hückel theory via Eq. (2) to calculate the resulting free energy difference ($\Delta\Delta G_{+-}^*$) to creating a charged species (*) within the anionic and cationic capsules:

$$\Delta \Delta G_{+-}^* = \frac{\delta q(q_- - q_+)}{\varepsilon R(1 + \kappa R)} \tag{2}$$

where δq is the charge of the guest (-1e), q_- and q_+ is the charge on the capsule, ε is the dielectric of the solvent (= 78); the dielectric of the inner space of the model (ε = 1) is implicit in Eq. (2)), κ^{-1} = 6.8 Å is the Debye length for the bulk mixture with 200 mM added monovalent electrolyte (NaOH), and R is the mean Born radius of the positively and negatively charged spherical hosts within the context of the continuum dielectric model (12.0 Å). The free energy difference for a species of formal charge minus one in the anionic and cationic capsules determined based on this expression is $\Delta\Delta G_{+-}^*$ = 17.2 kJ mol⁻¹, differing from that for the cyclization of guest **2a** by 3.2 kJ/mol (Table 2). This free energy difference corresponds to a p K_a shift between the capsules of 3.0, which again is in reasonable agreement with those reported (Figure 3). Overall, these agreements are excellent given the inherent assumptions made in this simple model, not least of which is the neglect of ion-specific binding to the outside of the two capsules. Furthermore, the model confirms the primary role of Coulombic forces in promoting cyclizations within the capsules.

Conclusions

We have reported on the ability of two supramolecular capsules to encapsulate and cyclize guests. These capsules have identical inner-spaces that only differ in the electrostatic potential field that envelops them: one positive, one negative. We find that relative to the negatively charged capsule, the positively charged host increases the acidity of bound guests and increases the rate of cyclization reactions involving a negatively charged transition state. Calculations

confirm that Coulombic forces are the primary reason for this, and that Born spheres are reasonable approximations of these nano-scale hosts. Surprisingly, our findings also show that the TS for cyclization is stabilized more in the positive capsule than simple guest deprotonation, suggesting that the non-polar pocket possesses functionality – beyond the simple EP field – that stabilizes the TS. We are continuing to investigate reactions within these two capsules to identify design criteria for nano-reactors.

Acknowledgements

BCG, KW and XC would like to thank the National Science Foundation for award CHE-1807101. HSA and BCG gratefully acknowledge the National Science Foundation (CBET-1403167 and CBET-1805167). Many thanks also to Dr. Jake Jordan for MALDI measurements and Sam Gellman for helpful discussions.

Reference

- 1. Petsko G. A., Ringe D. Protein Structure and Function. Sunderland, MA: New Science Press; 2004.
- 2. Zhang X., Houk K. N. Why Enzymes are Proficient Catalysts: Beyond the Pauling Paradigm. Acc. Chem. Res., **2005**, 38, 379-85.
- 3. Warshel A., Sharma P. K., Kato M., Xiang Y., Liu H., Olsson M. H. *Electrostatic basis for enzyme catalysis*. Chem. Rev., **2006**, *106*(8), 3210-35.
- 4. Wolfenden R. Degrees of Difficulty of Water-Consuming Reactions in the Absence of Enzymes. Chem. Rev., **2006**, *106*(8), 3379-96.
- 5. Pocker Y., Buchholz R. F. *Electrostatic catalysis by ionic aggregates. II. Reversible elimination of hydrogen chloride from tert-butyl chloride and the rearrangement of 1-phenylallyl chloride in lithium perchlorate-diethyl ether solutions.* J. Am. Chem. Soc., **1970**, 92(13), 4033-8.
- 6. Shaik S., Mandal D., Ramanan R. *Oriented electric fields as future smart reagents in chemistry*. Nat. Chem., **2016**, *8*(12), 1091-8.
- 7. Brown C. J., Toste F. D., Bergman R. G., Raymond K. N. Supramolecular catalysis in metal-ligand cluster hosts. Chem. Rev., **2015**, *115*(9), 3012-35.
- 8. Vriezema D. M., Aragonès M. C., Elemans J. A. A. W., Cornelissen J. J. L. M., Rowan A. E., Nolte R. J. M. *Self-Assembled Nanoreactors*. Chem. Rev., **2005**, *105*, 1445-89.
- 9. Kataev E. A., Müller C. Recent advances in molecular recognition in water: artificial receptors and supramolecular catalysis. Tetrahedron, **2014**, 70, 137-67.
- 10. Yoshizawa M., Klosterman J. K., Fujita M. *Functional Molecular Flasks: New Properties and Reactions within Discrete, Self-Assembled Hosts.* Angew. Chemie Int. Ed., **2009**, *48*, 3418-38.
- 11. Assaf K. I., Nau W. M. *Cucurbiturils: from synthesis to high-affinity binding and catalysis*. Chem. Soc. Rev., **2015**, *44*(2), 394-418.
- 12. Meeuwissen J., Reek J. N. *Supramolecular catalysis beyond enzyme mimics*. Nat. Chem., **2010**, *2*(8), 615-21.
- 13. Breslow R., Dong S. D. *Biomimetic Reactions Catalyzed by Cyclodextrins and their Derivatives*. Chem. Rev., **1998**, 98, 1997-2011.
- 14. Mosca S., Yu Y., Gavette J. V., Zhang K. D., Rebek J., Jr. *A Deep Cavitand Templates Lactam Formation in Water*. J. Am. Chem. Soc., **2015**, *137*(46), 14582-5.
- 15. Masseroni D., Mosca S., Mower M. P., Blackmond D. G., Rebek J., Jr. *Cavitands as Reaction Vessels and Blocking Groups for Selective Reactions in Water*. Angew. Chem. Int. Ed. Engl., **2016**, *55*(29), 8290-3.
- 16. Restrop P., Rebek J., Jr. Reaction of Isonitriles with Carboxylic acids in a cavitand: Observation of Elusive Isoimide Intermediates. J. Am. Chem. Soc., **2008**, *130*(36), 11850-1.
- 17. Wu N. W., Rebek J., Jr. *Cavitands as Chaperones for Monofunctional and Ring-Forming Reactions in Water.* J. Am. Chem. Soc., **2016**.
- 18. Kaanumalle L. S., Gibb C. L. D., Gibb B. C., Ramamurthy V. *Controlling Photochemistry with Distinct Hydrophobic Nanoenvironments*. J. Am. Chem. Soc., **2004**, *126*(44), 14366-7.
- 19. Kaanumalle L. S., Gibb C. L. D., Gibb B. C., Ramamurthy V. A Hydrophobic Nanocapsule Controls the Photophysics of Aromatic Molecules by Suppressing Their Favored Solution Pathways. J. Am. Chem. Soc., **2005**, *127*(11), 3674-5.
- 20. Natarajan A., Kaanumalle L. S., Jockusch S., Gibb C. L. D., Gibb B. C., Turro N. J., et al. Controlling Photoreactions with Restricted Spaces and Weak Intermolecular Forces: Remarkable Product Selectivity during Oxidation of Olefins by Singlet Oxygen. J. Am. Chem. Soc., 2007, 129, 4132-3.

- 21. Gibb C. L. D., Sundaresan A. K., Ramamurthy V., Gibb B. C. *Templation of the Excited-State Chemistry of α-(n-Alkyl) Dibenzyl Ketones: How Guest Packing within a Nanoscale Supramolecular Capsule Influences Photochemistry*. J. Am. Chem. Soc., **2008**, *130*(12), 4069-80.
- 22. Nishioka Y., Yamaguchi T., Yoshizawa M., Fujita M. *Unusual* [2+4] and [2+2] *Cycloadditions of Arenes in the Confined Cavity of Self-Assembled Cages.* J. Am. Chem. Soc., **2007**, *129*, 7000-1.
- 23. Nishioka Y., Yamaguchi T., Kawano M., Fujita M. *Asymmetric (2+2) Olefin Cross photoaddition in a self-assembled host with remote chiral auxiliaries.* J. Am. Chem. Soc., **2008**, *130*, 8160-1.
- 24. Horiuchi S., Nishioka Y., Murase T., Fujita M. *Both* [2+2] and [2+4] additions of inert aromatics via identical ternary host–guest complexes. Chem. Commun., **2010**, 3460-2.
- 25. Murase T., Horiuchi S., Fujita M. *Naphthalene Diels-Alder in a Self-Assembled Molecular Flask*. J. Am. Chem. Soc., **2010**, *132*, 2866-7.
- 26. Iwasawa T., Mann E., Rebek J., Jr. *A Reversible Reaction Inside a Self-Assembled Capsule*. J. Am. Chem. Soc., **2006**, *128*(29), 9308-9.
- 27. Hong C. M., Kaphan D. M., Bergman R. G., Raymond K. N., Toste F. D. Conformational Selection as the Mechanism of Guest Binding in a Flexible Supramolecular Host. J. Am. Chem. Soc., **2017**, *139*(23), 8013-21.
- 28. Levin M. D., Kaphan D. M., Hong C. M., Bergman R. G., Raymond K. N., Toste F. D. Scope and Mechanism of Cooperativity at the Intersection of Organometallic and Supramolecular Catalysis. J. Am. Chem. Soc., **2016**, *138*(30), 9682-93.
- 29. Kaphan D. M., Levin M. D., Bergman R. G., Raymond K. N., Toste F. D. *A supramolecular microenvironment strategy for transition metal catalysis*. Science, **2015**, *350*, 1235-8.
- 30. Zhao C., Toste F. D., Raymond K. N., Bergman R. G. *Nucleophilic Substitution Catalyzed by a Supramolecular Cavity Proceeds with Retention of Absolute Stereochemistry*. J. Am. Chem. Soc., **2014**.
- 31. Wang Z. J., Brown C. J., Bergman R. G., Raymond K. N., Toste F. D. *Hydroalkoxylation Catalyzed by a Gold(I) Complex Encapsulated in a Supramolecular Host*. J. Am. Chem. Soc., **2011**. Epub 2011/04/27.
- 32. Brown C. J., Miller G. M., Johnson M. W., Bergman R. G., Raymond K. N. *High-Turnover Supramolecular Catalysis by a Protected Ruthenium(II) Complex in Aqueous Solution*. JACS, **2011**, *133*(31), 11964-6.
- 33. Pluth M. D., Bergman R. G., Raymond K. N. *The Acid Hydrolysis Mechanism of Acetals Catalyzed by a Supramolecular Assembly in Basic Solution*. J. Org. Chem., **2009**, *74*, 58-63.
- 34. Pluth M. D., Bergman R. G., Raymond K. N. Acid Catalysis in Basic Solution: A Supramolecular Host Promotes Orthoformate Hydrolysis. Science, **2007**, 316, 85-8.
- 35. Yoshizawa M., Tamura M., Fujita M. *Diels-Alder in Aqueous Molecular Hosts: Unusual Regioselectivity and Efficient Catalysis*. Science, **2006**, 312, 251-4.
- 36. Cullen W., Misuraca M. C., Hunter C. A., Williams N. H., Ward M. D. *Highly efficient catalysis of the Kemp elimination in the cavity of a cubic coordination cage*. Nat. Chem., **2016**, *8*(3), 231-6.
- 37. Shi Q., Mower M. P., Blackmond D. G., Rebek J., Jr. *Water-soluble cavitands promote hydrolyses of long-chain diesters*. Proc. Natl. Acad. Sci. U. S. A., **2016**, *113*(33), 9199-203.
- 38. Hooley R. J., Rebek J., Jr. *A Deep Cavitand Catalyzes the Diels-Alder Reaction of Bound Maleimides.* Org. Biomol. Chem., **2007**, *5*, 3631-6.
- 39. Crisostomo F. R. P., Lkedo A., Shenoy S. R., Iwasawa T., Rebek J., Jr. *Recognition and Organocatalysis with a Synthetic Cavitand Receptor.* J. Am. Chem. Soc., **2009**, *131*, 7402-10.

- 40. Kamioka S., Ajami D., Rebek J., Jr. *Autocatalysis and organocatalysis with synthetic structures*. Proc. Natl. Acad. Sci. U. S. A., **2010**, *107*, 541-2.
- 41. Zhang Q., Catti L., Kailac V. R. I., Tiefenbacher K. *To catalyze or not to catalyze:* elucidation of the subtle differences between the hexameric capsules of pyrogallolarene and resorcinarene. Chemical Science, **2017**, *8*, 1653-7.
- 42. Zhang Q., Tiefenbacher K. *Terpene cyclization catalysed inside a self-assembled cavity*. Nat. Chem., **2015**, *7*(3), 197-202.
- 43. Zhang Q., Tiefenbacher K. Hexameric Resorcinarene Capsule is a Bronsted Acid: Investigation and Application to Synthesis and Catalysis. J. Am. Chem. Soc., **2013**, 135(43), 16213-9.
- 44. Gibb C. L. D., Gibb B. C. Well Defined, Organic Nano-Environments in Water: The Hydrophobic Effect Drives a Capsular Assembly. J. Am. Chem. Soc., **2004**, 126, 11408-9.
- 45. Liu S., Whisenhunt-loup S. E., Gibb C. L. D., Gibb B. C. *An improved synthesis of 'octaacid' deep-cavity cavitand*. Supramol. Chem., **2011**, 23(6), 480-5.
- 46. Hillyer M. B., Gibb C. L. D., Sokkalingam P., Jordan J. H., loup S. E., Gibb B. C. Synthesis of Water-Soluble Deep-Cavity Cavitands. Org. Lett., **2016**, *18*(16), 4048-51.
- 47. Porel M., Jayaraj N., Kaanumalle L. S., Maddipatla M. V. S. N., Parthasarathy A., Ramamurthy V. *Cavitand Octa Acid Forms a Nonpolar Capsuleplex Dependent on the Molecular Size and Hydrophobicity of the Guest*. Langmuir, **2009**, *25*(6), 3473-81.
- 48. Ewell J., Gibb B. C., Rick S. W. Water inside a hydrophobic cavitand molecule. J. Phys. Chem. B, **2008**, *112*(33), 10272-9.
- 49. Sullivan M. R., Yao W., Tang D., Ashbaugh H. S., Gibb B. C. *The Thermodynamics of Anion Complexation to Nonpolar Pockets*. J. Phys. Chem. B, **2018**, *122*(5), 1702-13.
- 50. Sokkalingam P., Shraberg J., Rick S. W., Gibb B. C. *Binding Hydrated Anions with Hydrophobic Pockets*. J. Am. Chem. Soc., **2016**, *138*(1), 48-51.
- 51. Carnagie R., Gibb C. L. D., Gibb B. C. *Anion Complexation and The Hofmeister Effect*. Angew. Chem. Int. Ed., **2014**, *53*(43), 11498-500. doi: doi.org/10.1002/anie.201405796 PubMed PMID: 25196481.
- 52. Jordan J. H., Gibb C. L. D., Wishard A., Pham T., Gibb B. C. *Ion-Hydrocarbon and/or Ion-Ion Interactions: Direct and Reverse Hofmeister Effects in a Synthetic Host*. J. Am. Chem. Soc., **2018**, *140*(11), 4092-9.
- 53. Tang H., de Oliveira C. S., Sonntag G., Gibb C. L., Gibb B. C., Bohne C. *Dynamics of a supramolecular capsule assembly with pyrene*. J. Am. Chem. Soc., **2012**, *134*(12), 5544-7.
- 54. Wang K., Gibb B. C. *Mapping the Binding Motifs of Deprotonated Monounsaturated Fatty Acids and Their Corresponding Methyl Esters within Supramolecular Capsules.* J. Org. Chem., **2017**, 82, 4279–88.
- 55. Zhang K. D., Ajami D., Gavette J. V., Rebek J., Jr. *Alkyl groups fold to fit within a water-soluble cavitand*. J. Am. Chem. Soc., **2014**, *136*(14), 5264-6.
- 56. Choudhury R., Barman A., Prabhakar R., Ramamurthy V. *Hydrocarbons depending on the chain length and head group adopt different conformations within a water-soluble nanocapsule:* 1H NMR and molecular dynamics studies. J Phys. Chem. B, **2013**, 117(1), 398-407. Epub 2012/12/12.
- 57. Liu S., Russell D. H., Zinnel N. F., Gibb B. C. Guest packing motifs within a supramolecular nanocapsule and a covalent analogue. J. Am. Chem. Soc., **2013**, *135*(11), 4314-24. doi: 10.1021/ja310741q.
- 58. Asadi A., Ajami D., Rebek J., Jr.. Bent alkanes in a new thiourea-containing capsule. JACS, **2011**, *133*(28), 10682-4. Epub 2011/06/23.
- 59. Ko Y. H., Kim H., Kim Y., Kim K. *U-shaped Conformation of Alkyl Chains Bound to a Synthetic Host.* . Angew. Chem. Int. Ed., **2008**, *47*, 4106-9.

- 60. Shi Q., Masseroni D., Rebek J., Jr. *Macrocyclization of Folded Diamines in Cavitands*. J. Am. Chem. Soc., **2016**.
- 61. Sinqh A., Mehrotra A., Regen S. L. *High Yield Medium Ring Synthesis of Thiacycloalkanes*. Synth. Commun., **1981**, *11*(5), 409-11.
- 62. Mandolini L., Vontor T. *Ring-Closure Reactions.* 13.1 A Convenient Synthesis of Many-Membered Thiacycloalkanes. Synth. Commun., **1979**, 9(9), 857-61.
- 63. Choo Tan L., Pagni R. M., Kabalka G. W., Hillmyer M., Woosley J. *The macrocyclization reaction of terminal dibromoalkanes with sulfide on alumina. The use of a solid support as an alternative to the high dilution technique*. Tetrahedron Lett., **1992**, 33(50), 7709-12.
- 64. Bennett G. M., Gudgeon H. 356. The formation of large ring monosulphides from halogenated sulphides with extended carbon chains. J Chem. Soc., **1938**, (0), 1891-7.
- 65. Vigderman L., Manna P., Zubarev Eugene R. Quantitative Replacement of Cetyl Trimethylammonium Bromide by Cationic Thiol Ligands on the Surface of Gold Nanorods and Their Extremely Large Uptake by Cancer Cells. Angew. Chem. Int. Ed., **2011**, *51*(3), 636-41.
- 66. Tindale J. J., Ragogna P. J. *Highly fluorinated phosphonium ionic liquids: novel media for the generation of superhydrophobic coatings.* Chem. Commun., **2009**, (14), 1831-3.
- 67. Bidoggia S., Milocco F., Polizzi S., Canton P., Saccani A., Sanavio B., et al. *Fluorinated* and Charged Hydrogenated Alkanethiolates Grafted on Gold: Expanding the Diversity of Mixed-Monolayer Nanoparticles for Biological Applications. Bioconjug. Chem., **2017**, 28(1), 43-52.
- 68. Alloway D. M., Graham A. L., Yang X., Mudalige A., Colorado R., Wysocki V. H., et al. Tuning the Effective Work Function of Gold and Silver Using ω-Functionalized Alkanethiols: Varying Surface Composition through Dilution and Choice of Terminal Groups. J Phys. Chem. C, **2009**, 113(47), 20328-34.
- 69. Jaiswal A., Rajagopal D., Lakshmikantham M. V., Cava M. P., Metzger R. M. *Unimolecular rectification of monolayers of CH3C(O)S-C14H28Q+-3CNQ- and CH3C(O)S-C16H32Q+-3CNQ- organized by self-assembly, Langmuir-Blodgett, and Langmuir-Schaefer techniques.* Phys. CHem. Chem. Phys, **2007**, *9*(30), 4007-17.
- 70. For example, whereas guests **2a-2c** formed 90-100% complex and guests **3a-3c** formed ~80% complex, **4a** and **4b** only formed ~50% complex, and only ~20% of **5** was encapsulated by **1b**. We attribute this phenomenon to the weaker hydration of trimethyl ammonium groups verses carboxylates ($\Delta H_{hyd} = -218$ and -425 kJ mol⁻¹ respectively), which results in poorer charge shielding and hence greater Coulombic repulsion between the pair of cavitands forming a capsule.
- 71. Barnett J. W., Gibb B. C., Ashbaugh H. S. Succession of Alkane Conformational Motifs Bound within Hydrophobic Supramolecular Capsular Assemblies. J. Phys. Chem. B, **2016**, 120(39), 10394-402.
- 72. Ohloff G., Pickenhagen W., Kraft P. Scent and Chemistry: The Molecular World of Odors. Germany: Wiley-VCH; 2012.
- 73. Laughton P. M., Robertson R. E. Solvent isotope effects for equilibria and reactions. Solute-solvent Interactions. New York: Marcel Dekker; 1969.
- 74. Wishard A., Gibb B. C. *Dynamic light scattering studies of the effects of salts on the diffusivity of cationic and anionic cavitands*. Beilstein J. Org. Chem., **2018**, *14*, 2212-9.